

Direct Current Sputtering Deposition of the Metallic Ceramic Ti_3SiC_2 Thin Film with Improved Hydrophobicity and Reduced Surface Energy

Hamdi Muhyuddin Barra^{1*} , and Henry J. Ramos²

¹Department of Physics, College of Natural Sciences and Mathematics, Mindanao State University - Main, Marawi City, Philippines

²National Institute of Physics, University of the Philippines – Diliman, Quezon City, Philippines

*Email Correspondence: hamdimuhyuddin.barra@msumain.edu.ph

Abstract

Metallic ceramic compounds, such as Ti_3SiC_2 , are innovative materials that combine the properties of metals and ceramics. However, most methods used in synthesizing these materials employ high deposition temperatures. Hence, in this work, Ti_3SiC_2 thin film was prepared and deposited on a steel sample without heating or biasing using a magnetized sheet plasma source. The synthesis was carried out by sputtering titanium, silicon, and graphite targets with Ar plasma at different deposition times of 60, 90, and 120 minutes. Energy dispersive X-ray (EDX) and X-ray diffraction (XRD) scans of the samples confirmed the synthesis of the desired compound. Moreover, the wettability and surface energy properties of the coated substrate were calculated by contact angle measurements. Results showed that as the deposition time increased, the coated substrate became more hydrophobic. Indeed, these findings show that Ti_3SiC_2 deposited steel substrate, with its increased hydrophobicity, is a potential self-cleaning coating for industrial tools.

Keywords: Contact angle, MAX phase, sputtering, surface energy, titanium silicon carbide

1.0 Introduction

Metallic ceramic, also called MAX phase, is a group of ternary compounds consisting of layered carbide or nitride (the X factor) with an early transition metal M and an A-group element. MAX-phase materials have excellent chemical, electrical, mechanical, and physical properties as they exhibit metallic and ceramic attributes (Barsoum, 2000; Rosli et al., 2019). They are electrically and thermally conductive, shock resistant, and damage tolerant at high temperatures like metals, as well as oxidation and corrosion resistant, thermally stable, and have high-melting temperature and low density like ceramics (Barsoum et al., 2000; Higashi et al., 2018; Shannahan et al., 2017). Hence, metallic ceramics

have caught the attention of materials scientists and researchers for their potential functional and industrial uses. In particular, the MAX phase is considered a promising structural material for high-temperature and nuclear applications (Tatarko et al., 2017).

The most studied of these ternary compounds is titanium silicon carbide (Ti_3SiC_2) (Dash et al., 2020; Eklund et al., 2010). This nanolaminate compound has the potential as a protective coating for industrial tools since it is thermally conductive, heat resistant, and free from emitting hazardous chemicals at high temperatures (Shi et al., 2020; Zhang et al., 2003). Accordingly, techniques such as physical vapor deposition,

chemical vapor deposition, and sintering methods synthesize Ti_3SiC_2 (Eklund et al., 2010; Jacques et al., 2010; Perevislov et al., 2021). In the physical vapor deposition of Ti_3SiC_2 , the most common method is sputtering techniques (Sonoda et al., 2013; Sun, 2011). Nonetheless, most of these methods are constrained by high deposition temperature requirements, which restricts the use of high-temperature sensitive materials (Barra & Ramos, 2011; Vishnyakov et al., 2013).

In this work, we report on the facile synthesis and deposition of Ti_3SiC_2 thin film at low deposition pressure. This innovative way was carried out via a magnetron-configured sheet plasma source, a sputtering system that does not necessitate substrate heating and biasing. Also, energy dispersive X-ray (EDX) and X-ray diffraction (XRD) spectroscopies were utilized to verify the effective synthesis of Ti_3SiC_2 . Moreover, to understand the surface properties of the Ti_3SiC_2 -coated samples, we calculated the surface energy and wetting properties of the samples using contact angle measurements.

2.0 Methods

Ti_3SiC_2 thin-film deposition

Synthesis of Ti_3SiC_2 was done using the sheet plasma negative ion source (SPNIS) with a magnetron configuration. Figure 1 shows the schematic diagram of the machine. In the production region, argon gas was introduced and ionized by ejected electrons from the tungsten filament. The generated plasma was then accelerated to the extraction region at a discharge current of 4 A and discharge potential of 50 V. Sheet plasma was produced due to the resultant effect of the two permanent Sm-Co magnets and Helmholtz coils. Titanium, silicon,

and graphite targets were placed near the bottom of the extraction chamber and were biased with a potential of negative 1000 V. Stainless steel type 316 substrate with dimensions $15 \times 15 \times 0.5 \text{ mm}^3$ was placed 2.5 cm above the target. Similar to previous studies employing the SPNIS, three samples were prepared with varying 60, 90, and 120-minute deposition times. All experimental runs were carried out under a constant gas-filling pressure of 6.0 mTorr. More importantly, the substrate was neither heated nor biased during the deposition process.

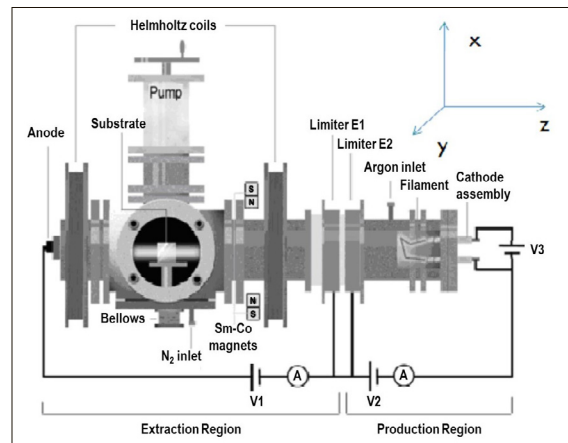


Figure 1. Schematic diagram of the SPNIS facility

After deposition, the sample was carefully taken out of the chamber and characterized using energy-dispersive X-ray spectroscopy (EDS) and X-ray diffractometry (XRD). EDS was employed to validate the presence of the three elements of the desired compound, while XRD was used to analyze the crystal structure and confirm the synthesis of Ti_3SiC_2 .

Contact Angle Measurements

The experimental setup in the measurement of static drop contact angle is illustrated in Figure 2.

A Dino-Lite digital microscope was focused on the cross-sectional view of the sample that was flatly positioned on a mount. With the aid of DinoCapture 2.0 software, the image was recorded on the embedded computer. Deionized water with constant volume was dropped on the surface of the sample. After five seconds, when the drop had settled on the solid surface, a picture was taken and saved on the computer. From the captured image, the three-point arc was used to measure the contact angle between the liquid and the surface.

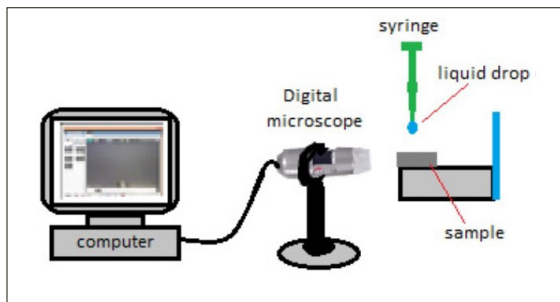


Figure 2. Experimental setup of contact angle measurement

Moreover, the measured contact angles were utilized to calculate the sample’s surface energy, which describes the wetting and adhesion properties of the sample. This was carried out by employing the van Oss-Chaudhury-Good technique (Xu et al., 1995; Zou et al., 2018). In this method, the total surface energy, γ_S , of a solid is given by

$$\gamma_S = \gamma_S^d + 2\sqrt{(\gamma_S^+)(\gamma_S^-)} \quad (1)$$

Where d represents the dispersive part of energy while + and – denote the acid and base adhesion parameters of the energy, respectively. Additionally, the solid energy parameters are related to the liquid energy, γ_L , and its components by

$$\left(\frac{1+\cos\theta}{2}\right)\gamma_L = \sqrt{\gamma_L^d\gamma_S^d} + \sqrt{\gamma_L^+\gamma_S^-} + \sqrt{\gamma_L^-\gamma_S^+} \quad (2)$$

where L stands for liquid and θ denotes the contact angle. Three liquids with known surface energies, as shown in Table 1, were employed to solve the solid energy parameters in equation (2). Deionized water, ethylene glycol, and glycerol were used as test liquids. Equation (2) then boiled down to a solvable three equations with three unknowns. Using Cramer’s rule for a 3x3 matrix, the values of the surface energy components of the solid in equation (2) were solved. These values were then directly substituted in equation (1) to get the sample’s total surface energy. Three trials were done for the contact angle measurements of each test liquid per sample to get more accurate results.

Table 1. Surface Energy Parameters of the Test Liquids

Test Liquid	γ_L (mJ/m ²)	γ_L^d (mJ/m ²)	γ_L^+ (mJ/m ²)	γ_L^- (mJ/m ²)
Deionized water	72.8	21.8	25.5	25.5
Glycerol	64	34	3.92	57.4
Ethylene glycol	48	29	1.92	17

After computations, the results were analyzed by comparing the values of the untreated and the Ti₃SiC₂-coated substrates.

3.0 Results and Discussion Structural Properties

All samples display metallic gray with shades of blue when taken out after the experimental runs, which implies thin-film deposition. The EDS result shown in Figure 3 validates the presence of the three elements (Ti, Si, and C) of the desired MAX

phase in the deposited substrate. Unlabeled peaks are inherent from the stainless-steel type 316.

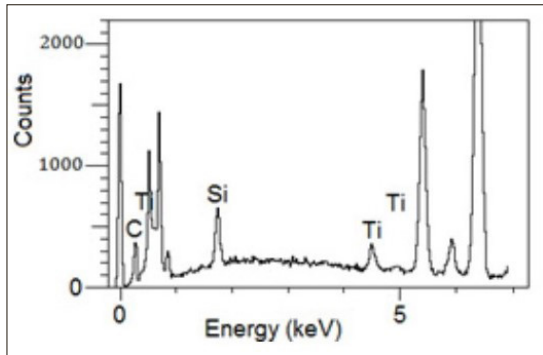


Figure 3. Energy dispersive X-ray spectrum of the coated substrate

The claim is further confirmed by the XRD results, as shown in Figure 4. The scans exhibit peaks at the 2θ -values of 10° , 39° and 79° , which match the (002), (104), and (10 $\bar{1}$ 3) phases of Ti_3SiC_2 , respectively. The peaks at around 45° and 65° correspond to the phases of Ti_5Si_3 , while the peak at $\sim 25^\circ$ matches the phase of the metal silicide TiSi . Unlabeled peaks are associated with the steel substrate. As seen the figure shows that the sample with the least deposition time exhibits the greatest peak intensity, which implies that it has the greatest Ti_3SiC_2 content. Further, it is observed that the intensity of the peaks associated with impurities decreased as the deposition time was increased.

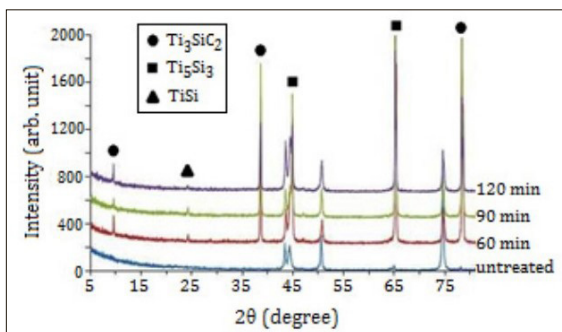


Figure 4. X-ray diffraction scan of the deposited substrates

Contact Angle and Surface Energy Measurements

The static drop contact angle measurements of deionized water to the Ti_3SiC_2 deposited surfaces show an increase in the hydrophobicity property of stainless steel, as illustrated in Figure 5. Also, as illustrated in Table 2, the average contact angle of the untreated substrate is 72.56° . Moreover, this is increased to 77.53° , 83.01° , and 96.43° in samples with deposition times of 60, 90, and 120 min, respectively. It is observed that as the deposition time increases, the substrate becomes more hydrophobic. Further, the maximum recorded contact angle is exhibited in the 120-min sample with a value of 97.64° .

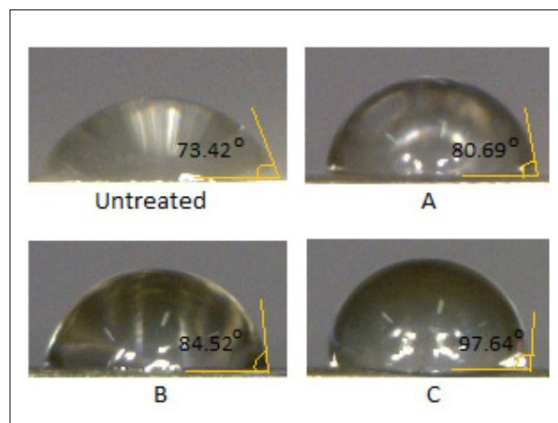


Figure 5. Static water drop contact angles of the substrates

Also listed in Table 2 are the complete values of the measured contact angles of the other test liquids. As seen, in glycerol, there is a decrease in the contact angles of the 60-min and 90-min samples but an increase in the 120-min sample. Meanwhile, in ethylene glycol, the contact angles of all samples are lower than the untreated substrate. Further, it can be observed that the 60-min sample showed the lowest value at 74.82° .

Based on the data in Table 1 and the average values of the angles listed in Table 2, the three

unknown solid surface energy components in Equation 2 were solved. The solutions were then directly substituted in Equation 1 to get the total surface energy of the substrate. Table 3 displays the results of the calculations. Consequently, the surface energy of the substrates decreased significantly after Ti_3SiC_2 coating. From an untreated surface energy of 75.36 mJ/m^2 , this was reduced to 28.82,

23.50, and 11.50 mJ/m^2 in the 60-, 90-, and 120-min samples, respectively. This finding conforms to the established principle that the lower the surface energy of a material, the greater the material's water contact angle (Güleç et al., 2006). Furthermore, the decrease in the deposited substrate's surface energy is brought about by a decrease in the substrate's dispersive energy component.

Table 2. Contact Angles between the Test Liquids and Substrate Surface

Sample	Deionized water, θ_1 ($^\circ$)				Glycerol, θ_2 ($^\circ$)				Ethylene glycol, θ_3 ($^\circ$)			
	Trial 1	Trial 2	Trial 3	Ave.	Trial 1	Trial 2	Trial 3	Ave.	Trial 1	Trial 2	Trial 3	Ave.
Untreated	72.32	73.42	71.93	72.56	66.61	66.55	66.55	66.57	98.75	99.46	99.25	99.15
60 min	80.69	76.04	75.85	77.53	52.66	52.52	52.03	52.41	73.69	75.14	75.63	74.82
90 min	84.52	83.54	80.97	83.01	50.99	48.54	50.56	50.03	81.94	81.47	78.69	80.70
120 min	95.61	96.04	97.64	96.43	71.26	72.65	72.34	72.08	94.63	89.42	88.29	90.78

Table 3. Calculated Total Surface Energy and Energy Components of the Samples

Sample	γ_s (mJ/m ²)	γ_s^d (mJ/m ²)	γ_s^+ (mJ/m ²)	γ_s^- (mJ/m ²)
Untreated	75.36	6.81	27.45	42.8
60 min	28.82	0.44	6.35	31.70
90 min	23.50	0.31	2.80	48.04
120 min	11.50	0.06	1.29	25.35

Finally, correlations of the static water contact angle, substrate surface energy, and deposition time are summarized and plotted in Figure 6. The figure shows the inverse proportionality relationship between contact angle and surface energy. More significantly, increasing the deposition time from 60 to 120 minutes increases the degree of water wetting and decreases the substrate's surface energy. These changes are possibly due to the high purity of the sample deposited at 120 min, as illustrated in the XRD scans in Figure 4. Additionally, the increased hydrophobicity and low surface energy of the third sample implies that Ti_3SiC_2 deposited stainless steel substrate has

potential application as a self-cleaning coating to industrial tools.

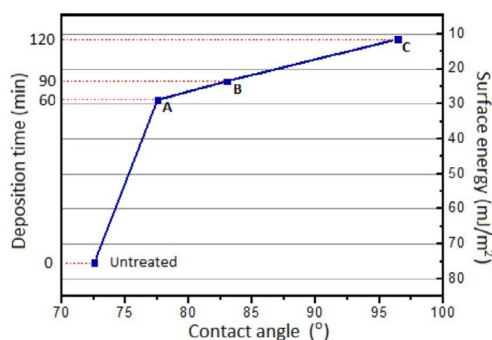


Figure 6. Correlations between the deposition time, surface energy, and the hydrophobicity of the substrates

4.0 Conclusions

Titanium silicon carbide (Ti_3SiC_2) was effectively synthesized using a magnetized sheet plasma source by sputtering Ti, Si, and graphite solids with Ar plasma. The thin film was deposited on a stainless steel substrate, which was neither heated nor biased. EDX and XRD scans confirm successful synthesis and deposition of the ternary compound as the Ti_3SiC_2 (002), (104), and (1013) facets were observed. Moreover, it is found that the intensity of the peaks decreases as the deposition time is prolonged.

In addition, the surface energy of the coated steel substrate was calculated using contact angle measurements. Results showed that the hydrophobicity of the coated substrate increased. Consequently, the surface energy of the deposited substrate decreased noticeably. Further, increasing the deposition time from 60 to 120 minutes caused a greater increase in the hydrophobicity of the substrate and a greater decrease in its surface energy. A maximum water contact angle value of 97.64° and minimum surface energy of 11.50 mJ/m^2 was observed with the most significant deposition time. The sample's improved hydrophobicity and low surface energy imply that it has potential as a self-cleaning coating. For future research, the synthesis of Ti_3SiC_2 coating can be carried out using different experimental parameters to increase further the hydrophobicity of the sample. Furthermore, characterization of the sample's surface topography, thermal conductivity, oleophobicity, and other properties can be studied to understand better the benefits of using Ti_3SiC_2 as a thin-film coating for industrial applications.

Acknowledgments

The authors would like to thank the Department of Science and Technology's Philippine Council

for Industry, Energy, and Emerging Technology Research and Development (DOST-PCIEERD) for the research grant.

References

- Barra, H. M. D., & Ramos, H. J. (2011). Deposition rate and energy enhancements of TiN thin-film in a magnetized sheet plasma source. *International Journal of Materials and Metallurgical Engineering*, 5(2), 114–116.
- Barsoum, M. W. (2000). The $\text{MN}_{n+1}\text{AX}_n$ phases: A new class of solids. *Progress in Solid State Chemistry*, 28(1-4), 201–281. [https://doi.org/10.1016/s0079-6786\(00\)00006-6](https://doi.org/10.1016/s0079-6786(00)00006-6)
- Barsoum, M. W., Yoo, H.-I., Polushina, I. K., Rud, V. Yu., Rud, Y. V., & El-Raghy, T. (2000). Electrical conductivity, thermopower, and hall effect of Ti_3AlC_2 , Ti_4AlN_3 , and Ti_3SiC_2 . *Physical Review B*, 62(15), 10194–10198. <https://doi.org/10.1103/physrevb.62.10194>
- Dash, A., Malzbender, J., Vaßen, R., Guillon, O., & Gonzalez-Julian, J. (2020). Short SiC fiber/ Ti_3SiC_2 MAX phase composites: Fabrication and creep evaluation. *Journal of the American Ceramic Society*, 103(12), 7072–7081. <https://doi.org/10.1111/jace.17337>
- Eklund, P., Beckers, M., Jansson, U., Högberg, H., & Hultman, L. (2010). The $\text{M}_{n+1}\text{AX}_n$ phases: Materials science and thin-film processing. *Thin Solid Films*, 518(8), 1851–1878. <https://doi.org/10.1016/j.tsf.2009.07.184>
- Güleç, H. A., Sarıoğlu, K., & Mutlu, M. (2006). Modification of food contacting surfaces by plasma polymerisation technique. Part I: Determination of hydrophilicity, hydrophobicity and surface free energy by contact angle method. *Journal of Food Engineering*, 75(2), 187–195. <https://doi.org/10.1016/j.jfoodeng.2005.04.007>
- Higashi, M., Momono, S., Kishida, K., Okamoto, N. L., & Inui, H. (2018). Anisotropic plastic deformation of single crystals of the MAX phase compound Ti_3SiC_2 investigated by micropillar compression. *Acta Materialia*, 161, 161–170. <https://doi.org/10.1016/j.actamat.2018.09.024>
- Jacques, S., Fakhri, H., & Viala, J.-C. (2010). Reactive chemical vapor deposition of Ti_3SiC_2 with and without pressure pulses: Effect on the ternary carbide texture. *Thin Solid Films*, 518(18), 5071–5077. <https://doi.org/10.1016/j.tsf.2010.02.059>
- Perevislov, S. N., Sokolova, T. V., & Stolyarova, V. L. (2021). The Ti_3SiC_2 max phases as promising materials for

- high temperature applications: Formation under various synthesis conditions. *Materials Chemistry and Physics*, 267, 124625. <https://doi.org/10.1016/j.matchemphys.2021.124625>
- Rosli, N. F., Nasir, M. Z. M., Antonatos, N., Sofer, Z., Dash, A., Gonzalez-Julian, J., Fisher, A. C., Webster, R. D., & Pumera, M. (2019). MAX and MAB phases: Two-Dimensional layered carbide and boride nanomaterials for electrochemical applications. *ACS Applied Nano Materials*, 2(9), 6010–6021. <https://doi.org/10.1021/acsnm.9b01526>
- Shannahan, L., Barsoum, M. W., & Lamberson, L. (2017). Dynamic fracture behavior of a MAX phase Ti_3SiC_2 . *Engineering Fracture Mechanics*, 169, 54–66. <https://doi.org/10.1016/j.engfracmech.2016.11.006>
- Shi, Q., Zhu, H., & Li, C. (2020). The effects of the addition of Ti_3SiC_2 on the microstructure and properties of laser cladding composite coatings. *Coatings*, 10(5), 498. <https://doi.org/10.3390/coatings10050498>
- Sonoda, T., Nakao, S., & Ikeyama, M. (2013). Deposition and characterization of MAX-phase containing Ti–Si–C thin films by sputtering using elemental targets. *Vacuum*, 92, 95–99. <https://doi.org/10.1016/j.vacuum.2012.02.004>
- Sun, Z. M. (2011). Progress in research and development on MAX phases: A family of layered ternary compounds. *International Materials Reviews*, 56(3), 143–166. <https://doi.org/10.1179/1743280410y.0000000001>
- Tatarko, P., Chlup, Z., Mahajan, A., Casalegno, V., Saunders, T. G., Dlouhý, I., & Reece, M. J. (2017). High temperature properties of the monolithic CVD β -SiC materials joined with a pre-sintered MAX phase Ti_3SiC_2 interlayer via solid-state diffusion bonding. *Journal of the European Ceramic Society*, 37(4), 1205–1216. <https://doi.org/10.1016/j.jeurceramsoc.2016.11.006>
- Vishnyakov, V., Lu, J., Eklund, P., Hultman, L., & Colligon, J. (2013). Ti_3SiC_2 -formation during Ti–C–Si multilayer deposition by magnetron sputtering at 650°C. *Vacuum*, 93, 56–59. <https://doi.org/10.1016/j.vacuum.2013.01.003>
- Xu, Z., Liu, Q., & Ling, J. (1995). An evaluation of the Van Oss-Chaudhury-Good equation and Neumann's equation of state approach with mercury substrate. *Langmuir*, 11(3), 1044–1046. <https://doi.org/10.1021/la00003a058>
- Zhang, Z.-F., Sun, Z. M., Hashimoto, H., & Abe, T. (2003). Fabrication and microstructure characterization of Ti_3SiC_2 synthesized from Ti/Si/2TiC powders using the pulse discharge sintering (PDS) technique. *Journal of the American Ceramic Society*, 86(3), 431–436. <https://doi.org/10.1111/j.1151-2916.2003.tb03317.x>
- Zou, W., Zhao, J., & Sun, C. (2018). Adsorption of anionic polyacrylamide onto coal and kaolinite calculated from the extended DLVO theory using the Van Oss-Chaudhury-Good theory. *Polymers*, 10(2), 113. <https://doi.org/10.3390/polym10020113>